JACS
JOURNAL OF THE AMERICAN CHEMICAL SOCIETY

Communication

pubs.acs.org/JACS

# Thin Films of Highly Planar Semiconductor Polymers Exhibiting Band-like Transport at Room Temperature

Jiyoul Lee,*[,†,‡] Jong Won Chung,[†] Do Hwan Kim,[#] Bang-Lin Lee,[†] Jeong-Il Park,[†] Sangyoon Lee,[†] Roger Häusermann,[∥] Bertram Batlogg,[∥] Sang-Soo Lee,[§,¶] Insil Choi,[⊥] Il Won Kim,[⊥] and Moon Sung Kang*[,⊥]

[†]Material Research Center, Samsung Advanced Institute of Technology, Suwon, Gyeonggi-do 443-803, Korea

[‡]Department of Graphic Arts Information Engineering, Pukyong National University, Busan 608-739, Korea

[#]Department of Organic Materials and Fiber Engineering, [⊥]Department of Chemical Engineering, Soongsil University, Seoul 156-743, Korea

[∥]Laboratory for Solid State Physics, ETH Zurich, Zurich 8093, Switzerland

[§]Photo-Electronic Hybrids Research Center, Korea Institute of Science and Technology, Seoul 136-791, Korea

[¶]KU-KIST Graduate School of Converging Science and Technology, Korea University, Seoul 136-701, Korea

Supporting Information

**ABSTRACT:** We report the observation of band-like transport from printed polymer thin films at room temperature. This was achieved from donor-acceptor type thiophene-thiazole copolymer that was carefully designed to enhance the planarity of the backbone and the resulting transfer integral between the macromolecules. Due to the strong molecular interaction, the printed polymer film exhibited extremely low trap density comparable to that of molecular single crystals. Moreover, the energy barrier height for charge transport could be readily reduced with the aid of electric field, which led formation of extended electron states for band-like charge transport at room temperature.

One of the key achievements in producing low-cost, high-performance organic electronics is achieving band-like transport from printed organic semiconductors. This transport behavior, characterized by increased charge carrier mobility upon lowering temperature, can be observed from highly crystalline semiconducting systems with suppressed energetic disorders. For polymer semiconductors, the achievement of this behavior has been considered challenging because of their inherent disorders arising from chain folding, entanglement, or torsion. Instead, thermally activated transport is typically observed from polymeric systems. Recent research accomplishments, however, including demonstration of extremely high carrier mobility >10 $cm^2\ V^{-1}\ s^{-1}$ and advanced understanding of structure-property relationships, lead researchers to anticipate that realizing practical polymer electronics devices relying on band-like transport may be within reach.[1−6]

The most fundamental and critical key for this goal is to enlarge the transfer integral between the macromolecules that determines the intermolecular charge transfer rate: the large transfer integral not only suppresses the influence of inherent disorders in the films but also leads to formation of extended energy states.[7,8] To enhance the transfer integral between macromolecules, the design rules for preparing new polymer systems rely on strategies that lead to (i) reducing $\pi$-$\pi$ stacking distances that would intensify intermolecular interactions and (ii) making the $\pi$-conjugated backbone units of the molecule planar so that the overlapping areas between $\pi$-orbitals become enlarged. The latter approach, in particular, is also known to benefit the intramolecular transport in polymers as the $\pi$-$\pi$ conjugation would be less hindered by twisting.[4,9,10] More recently, polymers in a donor-acceptor (*D-A*) configuration have been developed that exhibit large transfer integrals between macromolecules.[7] The compact molecular packing based on the *D-A* slipping packing mode and the resulting effective electronic coupling of these macromolecules yields efficient intermolecular transport.

In this report, we demonstrate a combined approach of the strategies presented above in designing semiconductor polymers, i.e., to make highly planar *D-A* polymers that can stack closer to each other with large intra- and intermolecular transfer integrals. A carefully designed thiophene-thiazole *D-A* polymer with minimal backbone rotation exhibited enhanced molecular interaction and suppressed electronic trap density compared to its sister polymers. Impressively, *inkjet printed* thin-films of the polymer exhibited room temperature band-like transport under a high electric field. In addition to the guidelines provided in this work for molecular design, we believe that these results set an important landmark for polymer electronics, particularly as they were attained under practical conditions: within reasonable device operation voltages, at room temperature, and from a conventional oxide-gated field-effect transistor platform through printing.

For the donor and acceptor units, thiophene and thiazole rings were employed, respectively.[8] Among various combinations of thiophene-thiazole semiconducting copolymer possible, we synthesized poly(tetryldodecyloctathiophene-*alt*-didodecylbithiazole) (**P8T2Z-C12**). The chemical structure of **P8T2Z-**

**Received:** April 24, 2015
**Published:** June 12, 2015





DOI: 10.1021/jacs.5b04253
*J. Am. Chem. Soc.* 2015, 137, 7990−7993

C12 is displayed in Figure 1a. For **P8T2Z-C12**, four thiophene rings without alkyl side chains were introduced into the

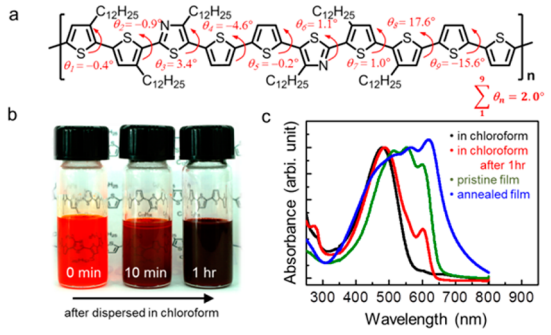


**Figure 1.** (a) Chemical structure of **P8T2Z-C12** depicted with twisted angle between consecutive aromatic rings. (b) Evolution of **P8T2Z-C12** dispersed in chloroform. (c) Absorbance spectrum for dispersion and thin films of **P8T2Z-C12**.

backbone, which were intended to serve as spacer groups when forming the slipping packing mode. Meanwhile, the position of the alkyl chains on the rest of the thiophene and thiazole rings was determined using molecular structure simulation (Materials Studio simulation software (version 7.0) from Accelrys) that provides the monomer unit with maximized planarity among various possible isomers. The monomer for the selected **P8T2Z-C12** structure in Figure 1a resulted in a total ring torsional angle, defined as the sum of the twisted angles between the consecutive aromatic rings, of ~2° over 10 subunits of subsequent thiophene and thiazole rings (Figure S3). This value is the minimal one among that of its sister DDADDA monomer units with different alkyl chain positions (Figures S2 and S4, Table S1). Also, this is substantially smaller than that of previously reported sister thiophene-thiazole copolymers (PQTBTz-C12)[11] and (PHTBTz-C12),[12] which was ~6−15° over six subunits of subsequent thiophene and thiazole rings (Figure S5). For comparison, a benchmark polythiophene, *regioregular* poly(3-hexylthiophene) (*rr*-P3HT), exhibits a torsional angle of ~70° over four subunits of thiophene rings.[13,14]

The intense molecular interaction of the as-designed polymers could be confirmed phenomenologically from their strong tendency to form aggregates when dispersed in conventional organic solvents. For example, the photographs in Figure 1b demonstrate the evolution of **P8T2Z-C12** dispersed in chloroform (1.0 wt %). The initially transparent dispersion of the polymers became turbid and dark with time, indicating the formation of polymer aggregates. Such a quick formation of aggregates is, indeed, a tell-tale indication of intense intermolecular $\pi$-$\pi$ interactions.[9,15] An even clearer evidence for the strong molecular interactions is provided from the absorbance spectra displayed in Figure 1c. After storing the polymer in chloroform for 1 h, a small red-shift (from 479 to 486 nm) in the absorbance maxima associated with the $\pi$-$\pi$* intraband transition was found. More noticeably, two additional peaks appeared at lower energies (~600 and ~570 nm), which can be assigned to vibronic structures, indicating a higher degree of ordering.[15] Interestingly, these vibronic peaks became even more prominent when the polymers formed films (green), and the enhancement was even more apparent when the films were annealed (blue). We emphasize that these vibronic peaks became higher than the peak assigned to the $\pi$-$\pi$* intraband transition, which was not observed from the sister copolymers (Figure S6). These features are attributed to the formation of crystalline aggregated domains of **P8T2Z-C12** either in chloroform or in solid thin films due to the strong molecular interaction of the planar copolymer.

The thin film structure of **P8T2Z-C12** prepared onto an octadecyltrichlorosilane (ODTS)-treated $SiO_2$/Si wafer was characterized using grazing incidence X-ray diffraction (GIXRD) measurements. The GIXRD patterns are shown in Figure S7a. The signals from the out-of-plane direction reveal multilayer nature of these films with an interlayer spacing of ~20 Å (Figure S7b). A consistent result was observed from atomic force microscopy (Figure S8). Additionally, well-ordered in-plane molecular packing showing an intermolecular stacking distance of ~3.69 Å was found (Figure S7c). This value is slightly smaller than the value for films of PQTBTz-C12 (3.70 Å)[16] and PHTBTz-C12 (3.75 Å).[12] Comparison of the physical parameters for these sister polymers is provided in Table S2.

The **P8T2Z-C12** thin films were used to form field-effect transistors (FETs) in a bottom contact, bottom gate configuration. We emphasize that the **P8T2Z-C12** was inkjet-printed onto an ODTS-treated glass wafer containing a plasma enhanced chemical vapor-deposited $SiO_2$ layer and prepatterned metal electrodes. The precise patterning of the active layer done by printing was critical not only for lowering the device off current but also for determining the area associated with the parasitic (specific) capacitance of the devices accurately. Both the low off current and the accurate parasitic capacitance value were necessary for the trap-density analysis described below.[17]

Figure 2a shows typical drain current-gate voltage ($I_D$-$V_G$) characteristics (the transfer characteristics) of an inkjet-printed

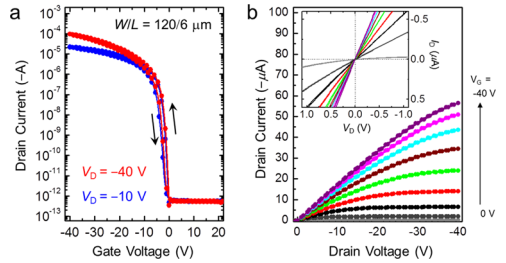


**Figure 2.** (a) Transfer characteristics of a **P8T2Z-C12** thin film FET measured at $V_D$'s of −10 V (blue) and −40 V (red). (b) Output characteristics of the FET measured at varying $V_G$'s. The inset shows the curves in near $V_D$ = 0 V.

**P8T2Z-C12** FET with channel length ($L$) and width ($W$) of 6 and 120 $\mu$m, respectively. These curves were obtained at fixed drain voltages ($V_D$) of −10 V (blue) and −40 V (red) under ambient conditions at room temperature. These values of $V_D$ correspond to the linear and saturation voltage regimes of transistors, respectively (the $I_D$-$V_D$ characteristics or the output characteristics are shown in Figure 2b). $I_D$ increased more than 8 orders of magnitude upon increasing $V_G$ negatively, yielding linear ($\mu_{lin}$) and saturation ($\mu_{sat}$) hole mobilities of 0.35 and 0.75 $cm^2\ V^{-1}\ s^{-1}$, respectively. The mobility values were obtained using standard transistor equations at respective operation regimes, as described in Figure S9. Additionally, the subthreshold swing was as low as 0.55 V $dec^{-1}$. These results along with the hysteresis-free *I-V* characteristics indicate minimal influence of traps.

The low density of traps for the inkjet-printed **P8T2Z-C12** films were quantified by simulating the transfer characteristics using a simulating program developed by Oberhoff et al.[18,19] The


DOI: 10.1021/jacs.5b04253
J. Am. Chem. Soc. 2015, 137, 7990−7993

simulation fits the density of trap states (trap DOS) to two exponential formulas that correspond to the shallow and deep trap levels, respectively. The resulting DOS for **P8T2Z-C12** thin-films are displayed in Figure 3 (black). The shallow trap DOS

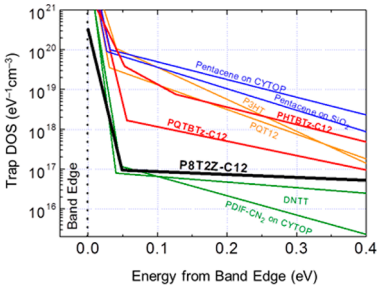


**Figure 3.** Trap DOS of a **P8T2Z-C12** thin film (black) extracted using a simulating program developed by Oberhoff et al.[18,19] Simulated results for reference samples are also shown.

located near the valence band edge (defined as $E$ = 0 eV) declined steeply from >$10^{20}$ to ~$10^{17}$ eV$^{-1}$ cm$^{-3}$ within the initial 50 meV from the edge. Over the next 0.4 eV, DOS corresponding to the deep levels varied rather gradually. For comparisons, the as-extracted DOS for its sister copolymers (PHTBTz-C12 and PQTBTz-C12 in red) and benchmark thiophene polymers (P3HT and poly(3,3‴-didodecylquaterthiophene) (PQT12) in orange) are displayed together in the plot.[17] The trap DOS in **P8T2Z-C12** is 1-3 orders of magnitude lower than that of the reference polymers. It is even 3 orders of magnitude lower than that in evaporated pentacene films (blue)[20] and is as low as in the best organic single crystals such as *N*,*N*′-bis(*n*-alkyl)-(1,7 and 1,6)-dicyanoperylene-3,4:9,10 bis(dicarboximide) (PDIF-CN2) and dinaphtho[2,3-*b*:2′,3′-*f*]-thieno[3,2-*b*]thiophene (DNTT) (green).[17,19,21] This highlights that the **P8T2Z-C12** films exhibit an exceedingly low trap density which is, up to now, only thought to be possible for physical vapor transport grown organic single crystals.

Due to the ultralow trap density, the **P8T2Z-C12** films yielded a long average hopping length ($l$) of ~9.5 nm, according to the method described by Asadi et al.[22] (Figure S11). This length corresponds to tens of $\pi$-$\pi$ stacking units. More interestingly, the carrier mobilities of the films estimated under the same voltage conditions varied as the channel length of the devices was altered (Figure S13). In other words, the carrier mobility of the system depended strongly on the lateral electric field ($E$) (Figure 4a). Accordingly, a hole mobility as high as 2.2 cm$^2$ V$^{-1}$ s$^{-1}$ was achieved at $V_D$ = −80 V (i.e., $E$ = 2 × 10$^7$ V m$^{-1}$) from devices with $L$ = 4 $\mu$m (Figure 4b). We confirmed through the transmission line method that the contact resistance was not

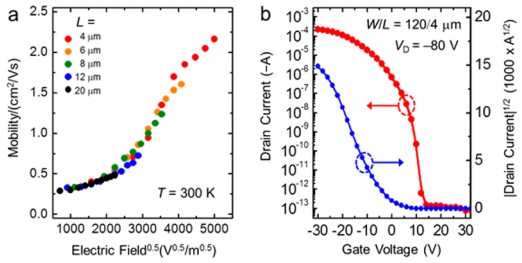


**Figure 4.** (a) A plot of mobility as a function of electric field collected from devices with varied channel length. (b) Transfer characteristics of a P8T2Z-C12 thin-film FET measured at $V_D$ = −80 V.

significant (<1.8 kΩ·cm), despite the short channel length of the devices (Figure S13). Additionally, the shape of the output characteristics near 0 V (the inset in Figure 2b) also supports that the device operation is not contact-dominant.

If not the contact issues, the results could then be explained by the critical role of the lateral electric field for transport in polymer thin films, known as the Poole-Frenkel effect.[23−25] According to the Poole-Frenkel model, the energy barrier between the localized states for a disordered system can be reduced by electric field, and thus, the resulting carrier mobility can be described with a relationship[26,27] $\mu = \mu_i \exp[\gamma\sqrt{E} - \Delta E/k_BT]$, where $\gamma = \beta_{PF}[1/k_BT - 1/k_BT_0]$ . Here, $\mu_i$ is the pre-exponential factor corresponding to the intrinsic mobility at the zero hopping barrier, $k_B$ is the Boltzmann constant, $\Delta E$ is the average barrier height for hopping process, $\beta_{PF}$ is the Poole-Frenkel constant, and $T_0$ is an empirical constant.[27] The $\beta_{PF}$ value for the **P8T2Z-C12,** which reflects the efficacy of lowering of the potential barrier in a Poole-Frenkel manner, was estimated to be 11.2 × 10$^{-5}$ eV(m/V)$^{1/2}$ (Figure S14). This is by far larger than any values reported for organic semiconductor systems (see Table S3). This indicates that the energy barriers for **P8T2Z-C12** can be effectively reduced with the aid of electric fields, which, in turn, led to the apparent field-dependent mobility.

As the barrier energies were reduced effectively by means of electric fields for **P8T2Z-C12** films, we then examined whether band-like transport based on extended energy states is realizable from these systems. This examination was performed experimentally by monitoring mobility values at varying temperatures (290-330 K)[28] and lateral electric fields (1.7 × 10$^6$ ~ 1.7 × 10$^7$ V m$^{-1}$) (Figure 5a). Under low electric fields ($E$ < 6.7 × 10$^6$ V

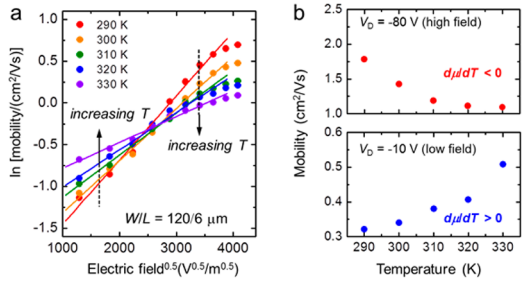


**Figure 5.** (a) Temperature-dependent Poole-Frenkel plot of mobility for printed **P8T2Z-C12** thin film. (b) Summary of temperature-dependent hole mobility obtained under high drain field ($V_D$ = −80 V, top) and low drain field ($V_D$ = −10 V, bottom).

m$^{-1}$), carrier mobility for **P8T2Z-C12** was suppressed as the temperature was reduced (d$\mu$/d$T$ > 0) (lower panel in Figure 5b and Figure S15). This is a typical indication of a thermally activated hopping transport, implying that the charge transport still takes place through a thermally assisted process under these low field conditions, despite the low density of trap states present in the system. When a high $E$ larger than 6.7 × 10$^6$ V m$^{-1}$ was applied, a negative mobility-temperature correlation (d$\mu$/d$T$ < 0), a signature of band-like transport, was attained (upper panel in Figure 5b).

Such an interesting transitional behavior can be explained qualitatively by extending the Poole-Frenkel model to the high-field limit. Beyond the explanation for the lowering of the barrier between localized energy states for a disordered system done by electric field, the model even anticipates that the barrier height can be completely negated when high enough $E = E_c$ is applied (so that the exponent in the Poole-Frenkel formula becomes zero



DOI: 10.1021/jacs.5b04253
J. Am. Chem. Soc. 2015, 137, 7990−7993

or $E = E_c = [\Delta E/(\gamma k_B T]^2)$. In fact, the achievement of a zero-height potential barrier was demonstrated experimentally for pentacene polycrystalline films when high enough $E$ is applied.[29] Considering the large $\beta_{PF}$ value for **P8T2Z-C12**, the negation of the energy barriers must be done very effectively. Accordingly, we consider that the observation of the negative mobility-temperature correlation from **P8T2Z-C12** is the result of applying electric field beyond the $E_c$. Under such conditions, the energy barrier that originally localizes the charge carriers would be removed. Consequently, the carrier transport in this regime can take place through extended energy states, which is now hampered rather than assisted by thermal energy that only amplifies lattice vibrations and carrier scattering.[30] Overall, we attribute the unique transport properties of the **P8T2Z-C12** films first to the highly planar backbone structure with large $l$ separated by potential barriers and second to the effectively reduced energy barriers (largest $\beta_{PF}$ value reported so far) through electric field in these films.

In conclusion, we demonstrated unique charge transport properties of inkjet printed films of **P8T2Z-C12**, a carefully designed polymer to enhance the intermolecular transfer integral. The planar *D-A* structure of the macromolecule yielded significant molecular interactions that led to polycrystalline films with ultralow trap densities. The disorders presented in these films could be negated effectively with the aid of electric fields, which allowed observing band-like transport from inkjet printed polymer films at room temperature. While further development of the transport model is necessary for quantitative description of the work, we believe that the results set an important step in printed polymer electronics; this is the first observation of electric field-driven negative mobility-temperature dependence for inkjet printed polymeric semiconductors near room temperature.

## ■ ASSOCIATED CONTENT

### Supporting Information

Material synthesis/characterization, structure simulation, film characterization, device fabrication/characterization, and DOS extraction. The Supporting Information is available free of charge on the ACS Publications website at DOI: 10.1021/jacs.5b04253.

## ■ AUTHOR INFORMATION


### Corresponding Authors

*jiyoul_lee@pknu.ac.kr
*mskang@ssu.ac.kr


### Notes

The authors declare no competing financial interest.

## ■ ACKNOWLEDGMENTS

This research was supported mainly by the Global Leading Technology Program of the Office of Strategic R&D Planning (OSP) funded by the Ministry of Commerce, Industry and Energy, Korea (No. 10042537), partially by the Basic Science Research Program of the National Research Foundation of Korea (NRF) funded by the Ministry of Education (NRF-2014R1A1A2058531), and partially by the Center for Advanced Soft-Electronics funded by the Ministry of Science, ICT and Future Planning of Korea as Global Frontier Project (CASE-2014M3A6A5060932).

## ■ REFERENCES


(1) Li, J.; Zhao, Y.; Tan, H. S.; Guo, Y.; Di, C.-A.; Yu, G.; Liu, Y.; Lin, M.; Lim, S. H.; Zhou, Y.; Su, H.; Ong, B. S. *Sci. Rep.* **2012**, *2*, 754.
(2) Kang, I.; Yun, H.-J.; Chung, D. S.; Kwon, S.-K.; Kim, Y.-H. *J. Am. Chem. Soc.* **2013**, *135*, 14896.
(3) Tseng, H.-R.; Phan, H.; Luo, C.; Wang, M.; Perez, L. A.; Patel, S. N.; Ying, L.; Kramer, E. J.; Nguyen, T.-Q.; Bazan, G. C.; Heeger, A. J. *Adv. Mater.* **2014**, *26*, 2993.
(4) Noriega, R.; Rivnay, J.; Vandewal, K.; Koch, F. P. V.; Stingelin, N.; Smith, P.; Toney, M. F.; Salleo, A. *Nat. Mater.* **2013**, *12*, 1038.
(5) Yuen, J. D.; Menon, R.; Coates, E. N.; Namdas, B. E.; Cho, S.; Hannahs, S. T.; Moses, D.; Heeger, A. J. *Nat. Mater.* **2009**, *8*, 572.
(6) Yamashita, Y.; Tsurumi, J.; Hinkel, F.; Okada, Y.; Soeda, J.; Zajączkowski, W.; Baumgarten, M.; Pisula, W.; Matsui, H.; Müllen, K.; Takeya, J. *Adv. Mater.* **2014**, *26*, 8169.
(7) Dong, H.; Fu, X.; Liu, J.; Wang, Z.; Hu, W. *Adv. Mater.* **2013**, *25*, 6158.
(8) Osaka, I.; Zhang, R.; Sauvé, G. v.; Smilgies, D.-M.; Kowalewski, T.; McCullough, R. D. *J. Am. Chem. Soc.* **2009**, *131*, 2521.
(9) Zhao, K.; Khan, H. U.; Li, R.; Su, Y.; Amassian, A. *Adv. Funct. Mater.* **2013**, *23*, 6024.
(10) Choi, S. H.; Kim, B.; Frisbie, C. D. *Science* **2008**, *320*, 1482.
(11) Kim, D. H.; Lee, B.-L.; Moon, H.; Kang, H. M.; Jeong, E. J.; Park, J.-I.; Han, K.-M.; Lee, S.; Yoo, B. W.; Koo, B. W.; Kim, J. Y.; Lee, W. H.; Cho, K.; Becerril, H. A.; Bao, Z. *J. Am. Chem. Soc.* **2009**, *131*, 6124.
(12) Lee, J.; Chung, J. W.; Jang, J.; Kim, D. H.; Park, J.-I.; Lee, E.; Lee, B.-L.; Kim, J.-Y.; Jung, J. Y.; Park, J. S.; Koo, B.; Jin, Y. W.; Kim, D. H. *Chem. Mater.* **2013**, *25*, 1927.
(13) de Oliveira, M. A.; de Almeida, W. B.; dos Santos, H. F. *J. Braz. Chem. Soc.* **2004**, *15*, 832.
(14) Barta, P.; Dannetun, P.; Stafström, S.; Zagórska, M.; Proń, A. *J. Chem. Phys.* **1994**, *100*, 1731.
(15) Aiyar, A. R.; Hong, J.-I.; Nambiar, R.; Collard, D. M.; Reichmanis, E. *Adv. Funct. Mater.* **2011**, *21*, 2652.
(16) Jang, J.; Kim, J.; Bae, M.; Lee, J.; Kim, D. M.; Kim, D. H.; Lee, J.; Lee, B.-L.; Koo, B.; Jin, Y. W. *Appl. Phys. Lett.* **2012**, *100*, 133506.
(17) Häuserman, R. Ph.D. Thesis, ETH-Zürich, Swizterland, 2013.
(18) Oberhoff, D.; Pernstich, K. P.; Gundlach, D. J.; Batlogg, B. *IEEE Trans. Elec. Dev.* **2007**, *54*, 17.
(19) Xie, W.; Willa, K.; Wu, Y.; Häusermann, R.; Takimiya, K.; Batlogg, B.; Frisbie, C. D. *Adv. Mater.* **2013**, *25*, 3478.
(20) Häusermann, R.; Batlogg, B. *Appl. Phys. Lett.* **2011**, *99*, 083303.
(21) Willa, K.; Häusermann, R.; Mathis, T.; Facchetti, A.; Chen, Z.; Batlogg, B. *J. Appl. Phys.* **2013**, *113*, 133707.
(22) Asadi, K.; Kronemeijer, A. J.; Cramer, T.; Koster, L. J. A.; Blom, P. W. M.; Leeuw, D. M. d. *Nat. Commun.* **2013**, *4*, 1710.
(23) Dhoot, A. S.; Wang, G. M.; Moses, D.; Heeger, A. J. *Phys. Rev. Lett.* **2006**, *96*, 246403.
(24) Hamadani, B. H.; Richter, C. A.; Gundlach, D. J.; Kline, R. J.; McCulloch, I.; Heeney, M. *J. Appl. Phys.* **2007**, *102*, 043503.
(25) Worne, J. H.; Anthony, J. E.; Natelson, D. *Appl. Phys. Lett.* **2010**, *96*, 053308.
(26) Hill, R. M. *Philos. Mag.* **1971**, *23*, 59.
(27) Blom, P. W. M.; de Jong, M. J. M.; van Munster, M. G. *Phys. Rev. B* **1997**, *55*, R656−R659.
(28) At lower temperatures below 280 K, the mobility values extracted from devices applied with high electric fields exhibited a significant measurement-to-measurement deviation. This prevented conducting high-field measurements at an expanded temperature range.
(29) Wang, L.; Fine, D.; Basu, D.; Dodabalapur, A. *J. Appl. Phys.* **2007**, *101*, 054515.
(30) Sakanoue, T.; Sirringhaus, H. *Nat. Mater.* **2010**, *9*, 736.




DOI: 10.1021/jacs.5b04253
*J. Am. Chem. Soc.* 2015, 137, 7990−7993